

# HandMime: Sign Language Fingerspelling Acquisition via Imitation Learning

Federico Tavella<sup>1,2</sup> and Aphrodite Galata<sup>1</sup> and Angelo Cangelosi<sup>1</sup>

**Abstract**—Learning fine-grained movements is among the most challenging topics in robotics. This holds true especially for robotic hands. Robotic sign language acquisition or, more specifically, fingerspelling sign language acquisition in robots can be considered a specific instance of such challenge. In this paper, we propose an approach for learning dexterous motor imitation from videos examples, without the use of any additional information. We build an URDF model of a robotic hand with a single actuator for each joint. By leveraging pre-trained deep vision models, we extract the 3D pose of the hand from RGB videos. Then, using state-of-the-art reinforcement learning algorithms for motion imitation (namely, proximal policy optimisation), we train a policy to reproduce the movement extracted from the demonstrations. We identify the best set of hyperparameters to perform imitation based on a reference motion. Additionally, we demonstrate the ability of our approach to generalise over 6 different fingerspelled letters.

## I. INTRODUCTION

Robots are finding more and more applications in different scenarios, from industrial to domestic settings. Consequently, it became fundamental to find a new way to make robots perform a very wide range of different actions. One possibility is to hard code as many primitives as possible, but that requires a lot of resources. Moreover, it is very difficult to hard-code actions which take into account all the possible variations that can occur. Alternatively, one could use teleoperation in order to manipulate the robot and make it move as it suits. However, this approach requires: (i) a person who controls the robot and (ii) a wide array of different sensors [1] to capture different movements. A more practical and efficient approach would involve observing a tutor performing an action and learning to reproduce it, similarly to how people acquire certain skills. An example of such instance is **robotic sign language acquisition**. Sign language is a natural language that conveys a message through visual means, as opposed to spoken language that uses sound. As such, it requires people to perform specific gestures and facial expressions. Considering that, according to the World Federation of Deaf “there are more than 70 million deaf people worldwide” [2], and that according to WHO “by 2050 nearly 2.5 billion people are projected to have some degree of hearing loss and at least 700 million will require hearing rehabilitation” [3], it is clear that also machines need to learn how to convey messages using a medium different from sound. Some recent research started

approaching the problem, focusing on imitation [4] [5] or translation [6]. However, neither of these approaches enable the robot to build an *embodied* representation of different signs based on RGB data, as they focus on retargeting rather than learning, or use additional hardware.

Recently, Learning from Demonstrations (LfD) [7] or Learning from Observations (LfO) [8] gained huge popularity in the robotics community. For example, Yang et al. [9] teach a Baxter robot how to cook by “watching” YouTube videos, or Peng et al. [10] make a robotic dog learn how to move by imitating an actual robot. Similarly, [11] and [12] perform virtual character animation by teaching a virtual humanoid different skills based on motion capture data. One of the main differences between these approaches is that some of them focus on an objective, while others on copying the movements (i.e., one focuses on *what* to perform while the other on *how* to perform it). In addition, reinforcement learning-based approaches enable the agent to learn in a human-like fashion and to *acquire* an **embodied** representation of such skills.

We propose an imitation learning approach to fingerspelled sign language acquisition (namely *HandMime*) based on reinforcement learning, adapting [11] [12] approaches to a robotic hand. Our approach is illustrated in Figure 1. Firstly, we build an URDF model of a human hand to simulate an artificial hand using a physics engine [13] and perform parameter tuning to estimate the controller parameters. Secondly, we extract a 3D mesh of the hand from videos – which contains 3D coordinates and rotations – by exploiting a pre-trained vision model. Finally, we use reinforcement learning to estimate a policy which, comparing random movements with the reference motion, enables the simulated hand to imitate the original sign.

To summarise, the contributions of our research are manifold. We:

- 1) Introduce the problem of sign language acquisition in robots from an embodied perspective,
- 2) Provide a new model for a robotic hand, which opposed to the Shadow Dexterous Hand or other models has an actuator for each single joint, which will be released upon acceptance,
- 3) Provide a detailed methodology to perform the tuning of a PD controller based on a Bayesian approach,
- 4) Demonstrate the transferability of DeepMimic [11] approach to hand motion imitation, and
- 5) Demonstrate the possibility of acquiring fingerspelling skills via reinforcement learning based on RGB video examples.

This work was not supported by any organization

<sup>1</sup> Federico Tavella, Aphrodite Galata and Angelo Cangelosi are with Department of Computer Science, The University of Manchester, M13 9PL Manchester, The United Kingdom

<sup>2</sup> Corresponding author [federico.tavella@manchester.ac.uk](mailto:federico.tavella@manchester.ac.uk)

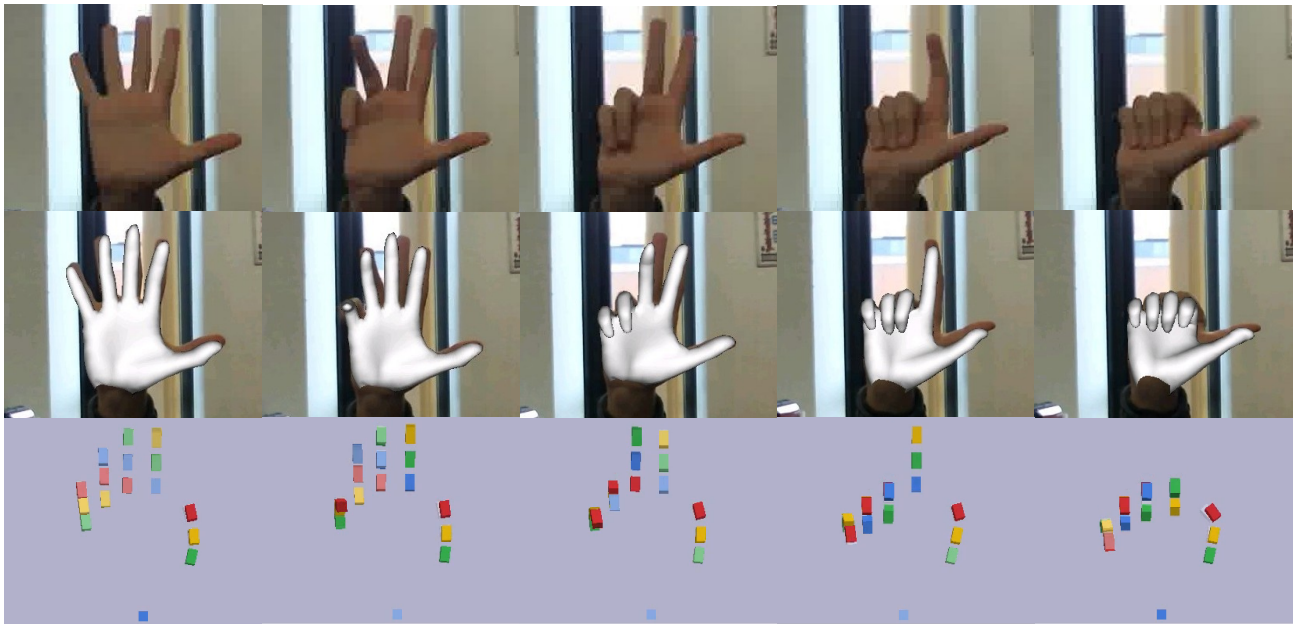


Fig. 1: HandMime extracts 3D coordinates and rotations from RGB videos using deep models. It then trains a policy using reinforcement learning, in order to teach to our robotic hand how to imitate the reference motion.

## II. RELATED WORK

### A. Learning from others

Behbahani et al. [14] learn models of behaviour from videos of traffic scenes collected from a monocular camera. More interestingly, LfD can be applied to control problems in order to teach virtual characters how to acquire different skills. One of the most relevant works in this direction is the one performed by Peng et al. [11], who build a virtual humanoid character who learns from motion capture data using reinforcement learning. Using this technique, the authors were able to teach a virtual character in a physical environment to perform different actions (e.g., walking, jumping, backflip). In addition, [10] applies the same approach to a simulated robotic dog instead of a humanoid and includes a domain adaptation part to transfer the policy to a physical robotic dog. [12] builds upon [11] integrating a video extraction and reconstruction pipeline to learn skills from videos in the wild. Similarly, Lee et al. [15] teach a simulated humanoid to perform different actions, but using a muscle-actuated human model instead of a motor-actuated one. [16] extract a controllable virtual character from a video of a person performing a certain action, like playing tennis. Finally, [17] overcome the necessity of manually designing imitation techniques for motion selection by using an automated approach which exploits adversarial imitation learning [18].

### B. RL and robotic hands

In addition to humanoid character control, reinforcement learning has been successfully applied to robotic and simulated hands. Most of the recent works use either the MIA hand or the Shadow dexterous hand [19]. Saito et al. [20] functionally mimic human grasps using a robotic hand and

reinforcement learning, develop a grasping reward, and apply domain randomisation to improve policy robustness. However, to perform grasping, it queries a library of grasping skills (i.e., a lookup table), so it actually takes advantage of a set of pre-defined grasping primitives. [21] use a motion capture glove combined with the MANO model [22] in order to collect data for objects manipulation. Then they perform optimisation of the finger joints (an inverse kinematics problem) to match the glove and MANO model keypoints. Finally, they transfer movements to the MIA and Shadow dexterous hands and perform simulation on PyBullet [13]. [23] use inverse kinematics to extract rotations from 3D keypoints in order to train a robotic hand. In addition, they exploit two existing datasets – BigHand2.2M [24] and the one introduced in [25] (captured with a haptic glove) – with ground truth in order to introduce an additional reward that encourages the policy to produce actions that resemble the user pose. Radosavovic et al. [26] propose state-only imitation learning (as opposed to standard state-action imitation learning) to address the lack of demonstration from which to learn skills, allowing learning from demonstrations coming from a different but related setting. [27] propose a novel demonstration-based method to convert human motion to robot demonstrations by extracting from videos 3D object and hand poses. However, while they exploit the MANO model, they use off-the-shelf skin segmentation and hand detection models to obtain a hand mask and an additional 2D pose estimator to extract the hand 2D keypoints and MANO parameters. Finally, they formulate the 3D hand joint estimation as an optimisation problem. They perform motion retargeting, while the fact that we predict rotations rather than keypoints means we do not require retargeting.

### C. Robotic sign language acquisition

Alabbad et al. [28] train a Pepper robot to recognise Arabic fingerspelled Arabic sign language letters and use natural language processing to translate written or spoken Arabic to sign language. Gago et al. [6] perform natural language to sign language translation in a human-robot interaction scenario. They combine sequence-to-sequence models to a lookup table to make a robot perform a series of signs – through retargeting and inverse kinematics – based on a corresponding written input sequence. Alternatively, Zhang et al. [4] use latent optimization to perform retargeting of Chinese sign language on three different virtual robots: YuMi, NAO, and Pepper. Hosseini et al. [5] teach to a RASA robot 10 different Persian signs using a mocap suit, mapping the user gestures to the robot joint space via interpolation and training a set of parallel Hidden Markov Models to encode each sign. This work is the one that resembles the most our approach, but it relies in additional hardware to capture signs. Additionally, it requires the demonstrator to repeat the sign until they are satisfied with the motion mirrored by the robot, introducing a possible bias regarding data acquisition (i.e., repeating the sign until the gesture performed by the robot is understandable).

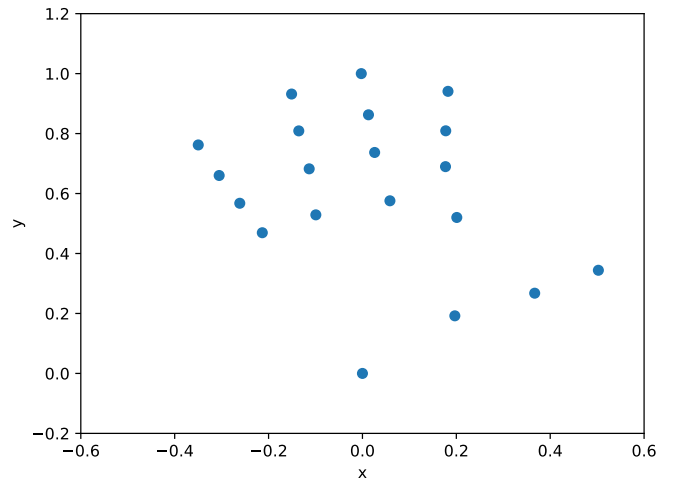
## III. METHODS

Our approach is composed of different stages, which we outline in the following sections. We start by describing how we build our hand model. We briefly explain how we use a deep learning model to extract information from RGB videos to imitate. Then, we describe how reinforcement learning can be used to motion imitation. Finally, we describe the problem we are tackling in terms of a Markov Decision Process.

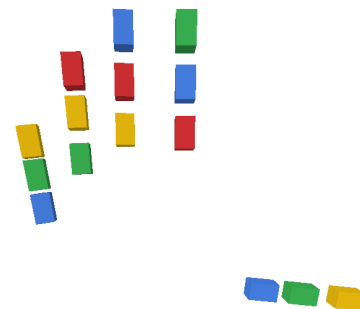
### A. Hand model

We build a model of a robotic hand based on the MANO model and the properties of a real human hand. To do so, we measure the position of the different joints of the hand and create an URDF model with the joints positioned accordingly. Figure 2 shows the reference keypoints (normalised based on maximum and minimum values for x and y) used to build the model and the respective URDF. Moreover, we impose realistic angular limitations to the joint of each finger.

Our robotic hand is made up of 5 fingers, where each finger is made up of 3 joints. For our purposes, we do not consider the wrist as a mobile joint as we focus on movements of the fingers. Moreover, we limit the movements of each finger joints to a single axis, as we believe it to be a reasonable approximation of how a human hand works. Thus, in total the model has 15 degrees of freedom (DoF). We impose a range limit for all the joints between  $[0, 2]$ , where 0 radians correspond to a fully-opened hand and 2 radians (i.e., slightly more than  $\pi/2$ ) to all the joints fully bent. We simulate the robotic hand using PyBullet [13], an open source physics simulator. For each joint motor, the simulated controller calculates the error as  $\varepsilon = k_p \Delta P + k_v \Delta V$  where  $k_p$  and  $k_v$  are, respectively, the position and velocity gains, and  $\Delta P = P - \hat{P}$  and  $\Delta V = V - \hat{V}$  are the position and velocity



(a) Normalised hand keypoints



(b) Hand URDF model

Fig. 2: We extract hand keypoints from a single frame and use them as reference to build the URDF model of our robotic hand.

errors (i.e., the difference between the desired and the actual value).

The only difference between our robotic hand and a human hand are the degrees of freedom and how the joints move. While in a finger, the joints are not independent (i.e., flexing one joint will cause other joints to flex as well), the joints in our robotic hand can move independently from each other.

*a) Motion extraction:* In order to extract motion from videos, we use FrankMocap [29], a single view 3D motion capture system. Taking an RGB image as input, it produces as output a 3D mesh based on the SMPL/SMPL-X [30] [31] models. In addition, it also provides 3D keypoints and joint rotations for both body and hands. Hence, we take advantage of this pre-trained model to extract joint rotations for each finger. As mentioned above, the joints of our robotic hand are capable of rotating along a single axis. Consequently, as the output of FrankMocap is expressed in axis-angle format, we discard the 2 additional angles.

## B. Motion imitation

Behavioral cloning is a technique in which human skills are observed and reproduced by a program [32]. From a technical point of view, there are several ways to perform behavioural cloning. The most straightforward technique is motion retargeting, in which a correlation between the observed and reproduced is established a priori. However, this approach requires hand-crafting and usually works only on the specific chosen model. A better approach should involve a learning component between the two models.

Reinforcement learning (RL) [33] has been widely applied to imitation learning and behavioural cloning. RL is usually formulated as a Markov Decision Process (MDP) [34], which has four main components: a set of states  $S$ , a set of actions  $A$ , a reward function  $R$ , and a policy  $\pi$ . A learning agent observes the environment and its own state  $s$ , and based on these observations (i.e., state) takes an action  $a$  to transition to a new state  $s'$  based on a probability

$$P_a(s, s') = Pr(s_{t+1} = s' | s_t = s, a_t = a) \quad (1)$$

which yields to a reward  $R_a(s, s')$  (i.e., an indicator of how good/bad was the chosen action). The final objective is to learn a policy – a mapping composed of actions chosen by the agent – which maximises the expected cumulative reward. Additionally, a policy can be parametric ( $\pi_\theta$ ). In this scenario, the policy has to find the optimal parameter  $\theta^*$  that maximises the expected cumulative reward. There are several algorithms that can be used to find an optimal policy. The algorithm is usually chosen based on the type of action and/or state spaces (discrete or continuous) or can be on-policy or off-policy. For more details, we redirect the reader to [33]. For our scenario, we use the Proximal Policy Optimisation (PPO) [35] algorithm to estimate a policy for our problem.

PPO is an optimisation algorithm used when both action and state spaces are continuous. It is a policy gradient method, where the gradient of the expected cumulative reward is calculated using trajectories  $\tau$  – i.e., sequences of  $(s, a, r)$  over a set of contiguous time steps – sampled by following the policy. Thus, given a parametric policy  $\pi_\theta$  and  $T$  steps, the expected reward is

$$J(\theta) = \mathbb{E}_{\tau \sim p_\theta(\tau)} \left[ \sum_{t=0}^T \gamma^t r_t \right] \quad (2)$$

where  $p_\theta(\tau) = p(s_0) \prod_{t=0}^{T-1} p(s_{t+1} | s_t, a_t) \pi_\theta(a_t | s_t)$  is the distribution over all possible trajectories  $\tau = (s_0, a_0, s_1, a_1, \dots, a_{T-1}, s_T)$  induced by the policy  $p_\theta$ ,  $p(s_0)$  being the initial state distribution and  $\gamma \in [0, 1]$  is a discount factor used to ensure that the reward has an upper bound. The policy gradient can be estimated as

$$\nabla_\theta J(\theta) = \mathbb{E}_{s_t \sim d_\theta(s_t), a_t \sim \pi_\theta(a_t | s_t)} [\nabla_\theta \log(\pi_\theta(a_t | s_t)) \mathcal{A}_t] \quad (3)$$

where  $d_\theta(s_t)$  is the distribution of states under the policy  $\pi_\theta$ , while  $\mathcal{A}_t = R_t - V(s_t)$  represents the advantage of taking

an action  $a_t$  from a given state  $s_t$ .  $R_t$  is the reward by a particular trajectory starting from state  $s_t$  at time  $t$ , and

$$V(s_t) = \mathbb{E}[R_t | \pi_\theta, s_t] \quad (4)$$

is the value function that estimates the average reward for starting at  $s_t$  and following the policy for all subsequent steps.

## C. Problem statement

We formulate the control problem of a robotic hand as a MDP. The action space is composed of different poses (i.e., combination of joint positions) for the controller, while the state describes a configuration of the hand, position and linear/angular velocity for each component of the hand. Moreover, a phase component  $\phi \in [0, 1]$  is added to the state space to synchronise the target and reference motions. We represent the policy using a multilayer perceptron with 2 hidden layers, which input and output dimensions are dictated by the space and action size, respectively. The number of hidden units for each layers is 1024, based on [11]. We estimate the pose error by calculating the scalar rotation of the quaternion difference between the simulated hand and the reference motion. In practise, this is similar to the mean squared error applied to quaternions. At time  $t$ , given the desired position  $p_{j,t}$  and the simulated position  $\hat{p}_{j,t}$  for joint  $j$ , the pose error is

$$\epsilon_t^p = \sum_j \|\hat{p}_{j,t} - p_{j,t}\|^2. \quad (5)$$

We calculate the velocity error  $\epsilon_t^v$  in the same manner, substituting the quaternions representing the pose with the velocities. Additionally, inspired by [11], we calculate an end effectors (i.e., fingertips) error  $\epsilon_t^e$  and a root error  $\epsilon_t^r$ . The former ensures that the 3D world position (in meters) of fingertips correspond, while the latter penalises deviations from root orientation when compared to the reference motion. Finally, the reward is calculated on the basis of the errors as follows

$$r_t = w^p r_t^p + w^v r_t^v + w^e r_t^e + w^r r_t^r \quad (6)$$

where  $w^x$  is a weight manually chosen (with the only condition of the different  $w^x$  summing to 1) and  $r_t^x$  is the reward at time-step  $t$  for the component  $x$ , calculated as  $r_t^x = e^{-k^x \epsilon_t^p}$  with  $k^x$  being a factor used to balance the reward based on the scale of the error. All the values for  $w$  and  $k$  are taken from [11]. As a proof-of-concept for our proposal, we train a policy for each different task. While it is not as efficient as training a single policy over different tasks, it enables us to easily evaluate the feasibility of our approach.

## IV. EXPERIMENTAL SETUP

We carry out three major experiments: one to tune the controller, one for searching hyperparameters, and another for training on the actual data. We use Weights and Biases [36] to carry out both the experiments for controller tuning and hyperparameters search. In particular, we use a

Bayesian approach instead of a grid search. In this way, the hyperparameters for the  $N + 1$  experiment are chosen on the basis of the results of the previous  $N$  runs. Additionally, we use Stable Baselines 3 [37] implementation of PPO.

### A. Controller tuning

Our controller can be tuned using two variables, namely  $k_p$  and  $k_d$ . Firstly, we generate a random reference motion which we use as a baseline for the tuning. Secondly, we create a function to minimise, which purpose is to make the reference motion and the simulated hand motion as similar as possible. We define this function as the sum of the pose and velocity errors  $\epsilon_t^p$  and  $\epsilon_t^v$

$$\epsilon^{control} = \epsilon_t^p + \epsilon_t^v \quad (7)$$

where  $\epsilon_t^p$  and  $\epsilon_t^v$  are defined according to Equation 5. This is because we want the simulated motion to resemble as much as possible the reference one, both in terms of *how* (i.e., pose) and *when* (i.e., velocity) the action is executed. Finally, we use a Bayesian optimisation strategy to find values that minimise  $\epsilon^{control}$ . To reduce the number of different simulations, we run 3 different swipes, characterised by different maximum values for the parameters  $k_p$  and  $k_d$ . The three different upper bounds are 100, 10 and 1 for both parameters.

### B. Motion imitation

Model selection and hyperparameters tuning are two fundamental steps in deep and reinforcement learning. However, due to the amount of resources necessary to perform a single training instance (approximately between 8 and 14 hours with 1 NVIDIA RTX 2080Ti GPU and 8 cores, depending on the parameters), we opt for a hierarchical approach.

In the first instance, we explore a subset of hyperparameters in order to understand how they affect training speed and performance. We acquire a reference motion used for the sole purpose of tuning, which can be found in the supplementary video. Table I lists all the different values we tried during our hyperparameters tuning. Finally, we test the ability of our tuned model to generalise by training a model - with the set of best hyperparameters identified during the previous step - over 6 different reference motions (i.e., fingerspelled letters A, B, C, D, E, F)<sup>1</sup>. We repeat each training session 10 times using different random seeds, in order to ensure statistical significance.

## V. RESULTS AND DISCUSSION

### A. Controller tuning

We briefly describe the results (providing Pearson correlation coefficient PCC [38] between the error and the parameters) and report the most relevant sweep.

Our first sweep is the one with the largest range: [0-100]. On one hand, there is no clear combination of values, which leads to a small error. However, it is noticeable that the runs leading to the lowest error are those in which  $k_d < k_p$

Parameter	Values
learning rate	(1, 3, 10, 30) x 10 <sup>-6</sup>
number of steps	512, 1024, 4096
weight decay rate	(1, 10) x 10 <sup>-5</sup>
batch size	128, 256, 512
orthogonal initialisation	true, false
discount factor	0.9, 0.95
log std dev	-3, -2, -1
number of epochs	3, 5, 10

TABLE I: Values of different hyperparameters explored during tuning.

(PCC 0.45 for  $k_d$  and -0.44 for  $k_p$ ), despite the fact that the error is very high. On the other hand, the sweep with the range [0, 10] clearly indicates that the values leading to the minimum error are the ones in the range [0, 2] (PCC 0.71 for both  $k_d$  and  $k_p$ ). Additionally, we can notice how the lowest values in the error scale are much lower to the ones of the previous sweep (86K vs 10K). Finally, Figure 3 gives us a compromise between the observations we made using the previous sweeps: the best results are obtained when  $k_d > k_p$  and with small values (PCC -0.49 for  $k_d$  and 0.51 for  $k_p$ ).

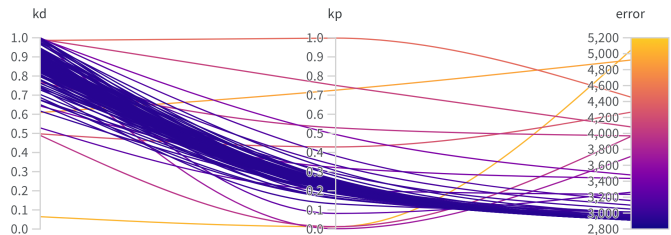


Fig. 3: Error for  $k_p$  and  $k_d$  with maximum values equal to 1

Finally, Figure 4 shows a comparison of the position and velocity of the reference and simulated motions of the last phalanx of the index finger, using the best values  $k_d = 0.87$  and  $k_p = 0.22$ .

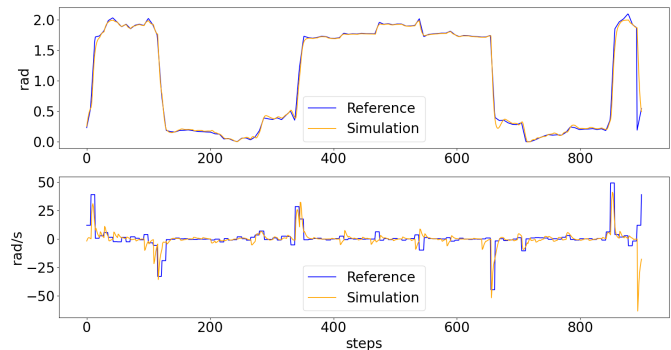


Fig. 4: Comparison between the reference and simulated position (left) and velocity (right) for the last phalanx of the index finger using the best couple of parameters.

<sup>1</sup><https://www.youtube.com/watch?v=tkMg8g8vVUo>

## B. Motion imitation

During our experiments, we found that no particular hyperparameter stood out for having a specific correlation, which yields a high reward. However, from Figure 5, it is clear that there is a huge difference between good and bad combinations of hyperparameters. In fact, we found out that the worst run (which leads to a mean reward of 854) uses the following values:  $batch\_size = 128$ ,  $gamma = 0.9$ ,  $learning\_rate = 10^{-5}$ ,  $log\_std\_init = -3$ ,  $n\_epochs = 10$ ,  $n\_steps = 1024$ ,  $ortho\_init = False$  and  $weight\_decay = 10^{-5}$ . On the opposite, the best run (mean reward equal to 1624) uses  $batch\_size = 128$ ,  $gamma = 0.9$ ,  $learning\_rate = 10^{-5}$ ,  $log\_std\_init = -2$ ,  $n\_epochs = 10$ ,  $n\_steps = 1024$ ,  $ortho\_init = False$  and  $weight\_decay = 10^{-5}$ . Hence, the only difference between the two runs is the value of the  $log\_std\_init$  parameter. Nevertheless, when we calculate the PCC between this parameter and the reward, we obtain a value of 0.081, indicating no clear linear correlation between the two values.

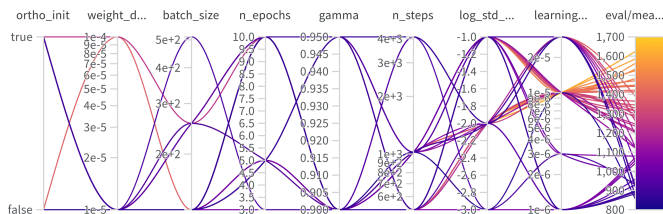


Fig. 5: Results of hyperparameter tuning across 50 different simulations.

Last but not least, we train our policies to imitate six different fingerspelled letters using the previously identified hyperparameters. Figure 6 illustrates the results of our training over 10 different seeds. All policies have a minimum value of 0.4 due to the normalised centre-of-mass reward being always 1, given that the hand as a whole is not moving from its initial position. Additionally, all the policies converge at most after 50 million steps. The normalised values for the reward vary between 0.8 and 0.95. Hence, we conclude that our model is able to learn different motions using the same model and hyperparameters. As additional evidence for this statement, we provide videos of the final results in the supplementary material, which can be used for a qualitative evaluation. Finally, we point out that the two dips in the reward curve for letter "F" in Figure 6 are due to two separate runs who present a single huge spike around 40 million and 50 million time steps respectively.

## C. Limitations

Our model is limited in terms of degrees of freedom. As a first approach, we chose to limit the DoFs to 1 for each joint. However, while this is correct for the distal and the proximal interphalangeal joints (i.e., the two outermost joints), this is not the case for the metacarpophalangeal joint. In particular, this constraint limits the mobility of the thumb. In addition, we limited wrist mobility, which is important for dexterous movements such as the one involved in sign language. All these physical limitations will be addressed in

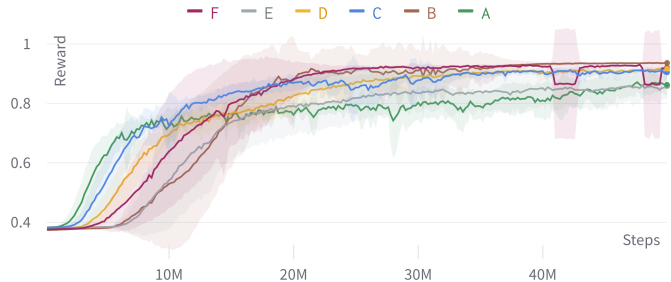


Fig. 6: Average and standard deviation for the reward of each different letter.

the next stage of our research by building upon our current model. Additional limitations are related to the learning algorithm we chose, and how we use it. First and foremost, reinforcement learning is known for being computationally expensive. In fact, we previously mentioned how a single run requires several hours. This shortcoming becomes even more relevant when we consider that we train a different policy for each different motion, as opposed to more efficient approaches that take advantage of motion priors [17] or mixture-of-experts. Nevertheless, recent progress in GPU-based simulations (e.g., NVIDIA Isaac sim [39]) and motion priors [17] can significantly speed up the learning process.

## VI. CONCLUSION AND FUTURE WORK

Our research focuses on the acquisition of sign language fingerspelling through imitation learning from RGB videos. This is a challenging task, as it requires the imitation of fine-grained movements. We developed an URDF model of a robotic hand, identified the parameters for the hand PD controller using a Bayesian approach and the hyperparameters for the imitation algorithm. In the end, we achieve imitation over 6 different fingerspelled letters. As future steps, we envision a new robotic hand with additional degrees of freedom, capable of imitating more complex motions. In addition, we plan to expand the evaluation to cover the entire fingerspelled alphabet and explore more efficient methodologies, such as mixture-of-experts [40] or motion priors [17]. HandMime could not only be used for scenarios in robotics (e.g., generation of grasping poses) but also for generating realistic animations for virtual characters. Ultimately, our goal is to achieve a fully functional model that can be tested and deployed on a physical robotic hand.

## ACKNOWLEDGMENT

For the purpose of open access, the author(s) has applied a Creative Commons Attribution (CC BY) license to any Accepted Manuscript version arising.

## REFERENCES

- [1] L. Penco, N. Scianca, V. Modugno, L. Lanari, G. Oriolo, and S. Ivaldi, "A multimode teleoperation framework for humanoid loco-manipulation: An application for the icub robot," *IEEE Robotics Automation Magazine*, vol. 26, no. 4, pp. 73–82, 2019.
- [2] "International day of sign language - un." <https://www.un.org/en/observances/sign-languages-day>. Accessed: 2022-08-23.

- [3] “Deafness and hearing loss - who.” <https://www.who.int/news-room/fact-sheets/detail/deafness-and-hearing-loss>. Accessed: 2022-08-23.
- [4] H. Zhang, W. Li, J. Liu, Z. Chen, Y. Cui, Y. Wang, and R. Xiong, “Kinematic motion retargeting via neural latent optimization for learning sign language,” *IEEE Robotics and Automation Letters*, vol. 7, no. 2, pp. 4582–4589, 2022.
- [5] S. R. Hosseini, A. Taheri, A. Meghdari, and M. Alemi, “Teaching persian sign language to a social robot via the learning from demonstrations approach,” in *international conference on social robotics*, pp. 655–665, Springer, 2019.
- [6] J. J. Gago, V. Vasco, B. Lukawski, U. Pattacini, V. Tikhonoff, J. G. Victores, and C. Balaguer, “Sequence-to-sequence natural language to humanoid robot sign language,” *ArXiv*, vol. abs/1907.04198, 2019.
- [7] A. Billard, S. Calinon, R. Dillmann, and S. Schaal, *Robot Programming by Demonstration*, pp. 1371–1394. Berlin, Heidelberg: Springer Berlin Heidelberg, 2008.
- [8] D. C. Bentivegna, C. G. Atkeson, and G. Cheng, “Learning tasks from observation and practice,” *Robotics and Autonomous Systems*, vol. 47, no. 2, pp. 163–169, 2004. Robot Learning from Demonstration.
- [9] Y. Yang, Y. Li, C. Fermuller, and Y. Aloimonos, “Robot learning manipulation action plans by “watching” unconstrained videos from the world wide web,” *Proceedings of the AAAI Conference on Artificial Intelligence*, vol. 29, Mar. 2015.
- [10] X. B. Peng, E. Coumans, T. Zhang, T.-W. Lee, J. Tan, and S. Levine, “Learning agile robotic locomotion skills by imitating animals,” 2020.
- [11] X. B. Peng, P. Abbeel, S. Levine, and M. van de Panne, “Deepmimic: Example-guided deep reinforcement learning of physics-based character skills,” *ACM Trans. Graph.*, vol. 37, pp. 143:1–143:14, July 2018.
- [12] X. B. Peng, A. Kanazawa, J. Malik, P. Abbeel, and S. Levine, “Sfv: Reinforcement learning of physical skills from videos,” *ACM Trans. Graph.*, vol. 37, Nov. 2018.
- [13] E. Coumans and Y. Bai, “Pybullet, a python module for physics simulation for games, robotics and machine learning,” 2016–2021.
- [14] F. Behbahani, K. Shiarlis, X. Chen, V. Kurin, S. Kasewa, C. Stirbu, J. Gomes, S. Paul, F. A. Oliehoek, J. Messias, and S. Whiteson, “Learning from demonstration in the wild,” in *2019 International Conference on Robotics and Automation (ICRA)*, pp. 775–781, 2019.
- [15] S. Lee, M. Park, K. Lee, and J. Lee, “Scalable muscle-actuated human simulation and control,” *ACM Trans. Graph.*, vol. 38, jul 2019.
- [16] O. Gafni, L. Wolf, and Y. Taigman, “Vid2game: Controllable characters extracted from real-world videos,” 2019.
- [17] X. B. Peng, Z. Ma, P. Abbeel, S. Levine, and A. Kanazawa, “Amp: Adversarial motion priors for stylized physics-based character control,” *ACM Trans. Graph.*, vol. 40, jul 2021.
- [18] J. Ho and S. Ermon, “Generative adversarial imitation learning,” 2016.
- [19] V. Kumar, Z. Xu, and E. Todorov, “Fast, strong and compliant pneumatic actuation for dexterous tendon-driven hands,” in *2013 IEEE International Conference on Robotics and Automation*, pp. 1512–1519, 2013.
- [20] D. Saito, K. Sasabuchi, N. Wake, J. Takamatsu, H. Koike, and K. Ikeuchi, “Task-grasping from human demonstration,” 2022.
- [21] A. Fabisch, M. Laux, D. Marschner, and J. Brust, “A modular approach to the embodiment of hand motions from human demonstrations,” 2022.
- [22] J. Romero, D. Tzionas, and M. J. Black, “Embodied hands: Modeling and capturing hands and bodies together,” *ACM Transactions on Graphics, (Proc. SIGGRAPH Asia)*, vol. 36, Nov. 2017.
- [23] G. Garcia-Hernando, E. Johns, and T.-K. Kim, “Physics-based dexterous manipulations with estimated hand poses and residual reinforcement learning,” in *2020 IEEE/RSJ International Conference on Intelligent Robots and Systems (IROS)*, pp. 9561–9568, 2020.
- [24] S. Yuan, Q. Ye, B. Stenger, S. Jain, and T.-K. Kim, “Bighand2.2m benchmark: Hand pose dataset and state of the art analysis,” 2017.
- [25] A. Rajeswaran, V. Kumar, A. Gupta, G. Vezzani, J. Schulman, E. Todorov, and S. Levine, “Learning Complex Dexterous Manipulation with Deep Reinforcement Learning and Demonstrations,” in *Proceedings of Robotics: Science and Systems (RSS)*, 2018.
- [26] I. Radosavovic, X. Wang, L. Pinto, and J. Malik, “State-only imitation learning for dexterous manipulation,” in *2021 IEEE/RSJ International Conference on Intelligent Robots and Systems (IROS)*, pp. 7865–7871, 2021.
- [27] Y. Qin, Y.-H. Wu, S. Liu, H. Jiang, R. Yang, Y. Fu, and X. Wang, “Dexmv: Imitation learning for dexterous manipulation from human videos,” 2021.
- [28] D. A. Alabbad, N. O. Alsaleh, N. A. Alaqeel, Y. A. Alshehri, N. A. Alzahrani, and M. K. Alhobaishi, “A robot-based arabic sign language translating system,” in *2022 7th International Conference on Data Science and Machine Learning Applications (CDMA)*, pp. 151–156, 2022.
- [29] Y. Rong, T. Shiratori, and H. Joo, “Frankmocap: A monocular 3d whole-body pose estimation system via regression and integration,” in *IEEE International Conference on Computer Vision Workshops*, 2021.
- [30] M. Loper, N. Mahmood, J. Romero, G. Pons-Moll, and M. J. Black, “SMPL: A skinned multi-person linear model,” *ACM Trans. Graphics (Proc. SIGGRAPH Asia)*, vol. 34, pp. 248:1–248:16, Oct. 2015.
- [31] G. Pavlakos, V. Choutas, N. Ghorbani, T. Bolkart, A. A. A. Osman, D. Tzionas, and M. J. Black, “Expressive body capture: 3D hands, face, and body from a single image,” in *Proceedings IEEE Conf. on Computer Vision and Pattern Recognition (CVPR)*, pp. 10975–10985, 2019.
- [32] C. Sammut, *Behavioral Cloning*, pp. 93–97. Boston, MA: Springer US, 2010.
- [33] R. S. Sutton and A. G. Barto, *Reinforcement Learning: An Introduction*. Cambridge, MA, USA: A Bradford Book, 2018.
- [34] R. Bellman, “A markovian decision process,” *Indiana Univ. Math. J.*, vol. 6, pp. 679–684, 1957.
- [35] J. Schulman, F. Wolski, P. Dhariwal, A. Radford, and O. Klimov, “Proximal policy optimization algorithms,” 2017.
- [36] L. Biewald, “Experiment tracking with weights and biases,” 2020. Software available from wandb.com.
- [37] A. Raffin, A. Hill, A. Gleave, A. Kanervisto, M. Ernestus, and N. Dornmann, “Stable-baselines3: Reliable reinforcement learning implementations,” *Journal of Machine Learning Research*, vol. 22, no. 268, pp. 1–8, 2021.
- [38] D. Freedman, R. Pisani, and R. Purves, “Statistics (international student edition),” *Pisani, R. Purves, 4th edn. WW Norton & Company, New York*, 2007.
- [39] “Nvidia isaac sim.” <https://developer.nvidia.com/isaac-sim>. Accessed: 2022-06-12.
- [40] J. Won, D. Gopinath, and J. Hodgins, “A scalable approach to control diverse behaviors for physically simulated characters,” *ACM Trans. Graph.*, vol. 39, jul 2020.